ELSEVIER

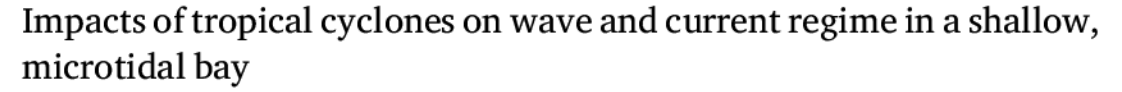
Contents lists available at ScienceDirect

# Continental Shelf Research

journal homepage: www.elsevier.com/locate/csr



## Research papers



Jay Merrill<sup>1</sup>, Giulio Mariotti, Chunyan Li, Matthew Hiatt\*

Department of Oceanography and Coastal Sciences, College of the Coast and Environment, Louisiana State University, LA, USA Coastal Studies Institute, Louisiana State University, LA, USA



Dataset link: https://doi.org/10.6084/m9.figsh are,25050038

Keywords: Currents Waves Circulation Tropical cyclones Hurricanes

## ABSTRACT

In shallow, microtidal coastal regions storms play a significant role in influencing wave climate and circulation patterns. In the northern Gulf of Mexico, understanding the effects of tropical cyclones on hydrodynamic processes is crucial for making predictions in the face of rapid wetland loss and increasing human interventions via restoration and protection strategies, such as river diversions. In this study, two bottom-mounted upward-facing Acoustic Current Doppler Profilers and separate wave recorders were installed in Barataria Bay (Louisiana, USA) to measure waves and current velocities responding to the passage of multiple tropical cyclones in fall 2020 and summer 2021. Analyses of depth-averaged current velocities suggest diurnal astronomic constituents drive currents over a 6-8 day period during and after storms, despite the microtidal nature of the bay. Wind-driven flow reversals of subtidal surface currents were observed during surge events. Storms that made landfall to the west of the bay resulted in enhanced subtidal current velocity magnitude during pre-and post-landfall periods while the one storm that made landfall to the east of the bay showed substantially less subtidal current response. Wave heights during storms are well reproduced by a semi-empirical model based on wind speed, fetch, and water depth, indicating that waves are locally generated. Tropical cyclones significantly influenced sub-tidal current velocities, depending on storm track and time of impact relative to the tidal cycle.

## 1. Introduction

Coastal Louisiana has been experiencing a land-loss crisis (Barras et al., 2003) in the face of eustatic sea-level rise and high rates of subsidence (Kolker et al., 2011; Yuill et al., 2009; Jankowski et al., 2017). A significant portion of the region is currently starved of allochthonous sediment due to isolation from the Mississippi River via levees (Paola et al., 2011). Low-lying coastal wetlands are also particularly vulnerable to erosion caused by wind waves and storm surge (Ortiz et al., 2017; Valentine and Mariotti, 2019; Palaseanu-Lovejoy et al., 2013). Tropical cyclones (TCs) can be significant contributors to land loss (Couvillion et al., 2011; Palaseanu-Lovejoy et al., 2013), and storm surge has been shown to enhance shallow tidal basin erosion along the marsh boundary (Mariotti et al., 2010). Not only are TCs and associated storm surge in the northern Gulf of Mexico (nGOM) projected to increase by 2100, but they are also predicted to disproportionately impact sediment-starved coastal bays (Camelo et al., 2020; Siverd et al., 2019). Shallow, sediment-depleted coastal areas in the nGoM can therefore act as a test bed for understanding the impacts of storms on coastal hydrodynamics in a rapidly degrading back-barrier environments, providing implications for coastal protection and restoration strategies.

It is understood that storm events impact circulation patterns and wave characteristics in microtidal systems, but there is a lack of observations targeting the hydrodynamic response to TCs within back-barrier estuaries in the nGOM. Previous studies of nearshore nGOM hydrodynamics responding to TCs focused on measuring and modeling the response of coastal currents to individual storms (Wilson et al., 2006; Guerra-Chanis et al., 2021), hindcast modeling of wave characteristics in response to known wind intensity (Zhao and Chen, 2008; Huang and Li, 2020), and measuring wave and current climate within open shelf waters or at the passes of an estuary (Allison et al., 2005; Sheremet et al., 2005; Li et al., 2009, 2010). It is not uncommon for multiple TCs to pass through the region in a given year (Miller and Trepanier, 2021). It follows that each event should uniquely perturb wave climate and current velocities within an open estuary, and the window over which the system returns to pre-storm conditions depends on TC magnitude,

<sup>\*</sup> Corresponding author at: Department of Oceanography and Coastal Sciences, College of the Coast and Environment, Louisiana State University, LA, USA. E-mail address: mhiatt1@lsu.edu (M. Hiatt).

<sup>&</sup>lt;sup>1</sup> Present address: School of Civil & Construction Engineering, Oregon State University, OR, USA.

direction, intensity, storm track, and the distance over which sustained winds persist (Bromirski and Kossin, 2008). Additionally, TCs that move over areas remote to the site of interest can significantly alter hydrodynamics within the system due to alteration of regional wind fields, among other factors. Given projections of more frequent and intense TCs (Webster et al., 2005) and an increased proportion entering the nGOM (Holland et al., 2010), such observations are important for assessing predictions in a changing climate. This paper addresses this issue by capturing the hydrodynamic responses to four TCs in Barataria Bay, Louisiana (Fig. 1) and the periods in between storms (i.e., quiescent periods).

The nGOM is affected by frequent TCs that cause disruptions to the typical nearshore hydrodynamic variability in the form of substantial storm surge (1-10 m) alongside increased wave heights (<1-2 m) (Muller and Stone, 2001; Georgiou et al., 2005; Hiatt et al., 2019). However, due to the destructive nature of TCs there is often limited data available of direct hydrodynamic impacts, much less for successive events. Barataria Bay is protected from the nGOM via barrier islands (see Fig. 1) and thus represents an attractive location for measurements. Research on current velocities within Barataria Bay is mainly restricted to the four main passes that exchange flows with the nGoM, being Caminada Pass, Barataria Pass, Pass Abel, and Ouatre Bayou (listed from west to east), which tidally exchange approximately 10%, 57%, 21%, and 12% of flow to and from the bay, respectively (Li et al., 2019; Payandeh et al., 2019). Additional pertinent research within Barataria Bay has been focused on numerical modeling of hydrodynamics (Huang and Li, 2020) and sediment dynamics (Mariotti et al., 2022). Li et al. (2021) studied hydrodynamics and sediment dynamics in the open water lower estuary of Barataria Bay during cold front season, however, current velocities were not taken into account and no major storm event was observed during the study. Thus, there is strong interest to quantify the disruptions to current velocities and wave characteristics induced

This study uses current velocity and wave data collected by Acoustic Doppler Current Profilers (ADCPs) and pressure transducers within the lower portion of Barataria Bay. The primary goal is to determine how waves and currents behave during both quiescent periods and when the bay is impacted by TCs. Analyses of time-varying wave height and direction, depth-averaged current (DAC) velocities, and the velocity profile response to storm events are the primary data products of this research. This work has implications for the considerable protection and restoration investments in the region aimed at mitigating wetland loss and protecting communities (e.g., CPRA, 2023).

### 2. Methods

## 2.1. Study site

Barataria Bay is an interdistributary bay that comprises the southern portion of the nearly 6300 km<sup>2</sup> Barataria Basin, situated along the southeastern coastline of Louisiana and to the south and west of the Mississippi River (Fig. 1). Water depth within the relatively flat open bay typically ranges between 1 and 3 m (Sorourian et al., 2020; Li et al., 2019). The long axis extends approximately 50 km from the mouth at Barataria Pass to the bay head at Bayou Perot and is oriented 340° from true north (Payandeh et al., 2019). Barataria Bay is separated from the nGOM by barrier islands, formed through the reworking of sediment previously deposited by a series of paleo-deltaic lobes of the Mississippi River (Hughes, 2016). The barrier islands are bisected by four main inlets that exchange flows with the nGOM over the Louisiana Shelf. Fluvial input into the bay is restricted to controlled freshwater discharge from the Mississippi River via the Davis Pond Freshwater Diversion Structure (DPFD), and flow from the east-west trending Gulf Intracoastal Waterway (GIWW). Measured flows between 2002 and 2018 at the DPFD averaged around 40 cubic meters per second (m<sup>3</sup>  $\rm s^{-1}$ ) but have been measured up to 610  $\rm m^3~s^{-1}$  (Ou et al., 2020; Turner

et al., 2019). Prior to the implementation of the freshwater diversion, discharge measured south of Bayou Perot (north of the open water portion of Barataria Bay) reached approximately 830 m<sup>3</sup> s<sup>-1</sup>, attributed to the GIWW (Swarzenski et al., 2003).

Barataria Bay experiences primarily diurnal tides characterized by  $O_1$ ,  $K_1$ , and  $P_1$  constituents, with periods of 25.82, 23.93, and 24.07 hr, respectively (Li et al., 2019, 2021), alongside tropical (maximal) and equatorial (minimal) tidal cycles. The system is microtidal (0.3 m average tidal range), and larger water level fluctuations are typically modulated by wind (Hiatt et al., 2019; Li et al., 2021; Valentine and Mariotti, 2019). Significant wave height  $(H_s)$  has been measured consistently at less than 1 m, and during quiescent periods typically remains below 0.4 m (Li et al., 2021; Sorourian et al., 2020). Salinity is spatially variable, ranging from near zero in the upper basin to approximately 23.0 psu at the tidal inlets (Ou et al., 2020). Between 1932 and 2016, Barataria Basin experienced a net land loss of more than 1,100 km<sup>2</sup>, roughly equivalent to 35% the land area of the state of Rhode Island Couvillion et al. (2011). Barataria Basin lost approximately 50 km<sup>2</sup> of land in 2004–2005 alone as a result of Hurricanes Katrina and Rita (FitzGerald et al., 2007). Accordingly, there is considerable restoration activity in the region aimed at preventing erosion and reversing wetland loss with land-building through sediment diversions, such as the Mid-Barataria Diversion Structure, which began construction in Fall 2023 (CPRA, 2023; LATIG, 2021; Xu et al., 2019).

#### 2.2. Data collection

Two open water locations within lower Barataria Bay were chosen to record wave and current information (Fig. 1). The northern and southern sites correspond to United States Geological Survey (USGS) water monitoring station 07380251 at 29°25'21.0"N, 89°57'02.0"W and USGS Station 073802514 at 29°20′1.05″N, 89°59′18.6″W (Fig. 1, BBN and BBS, respectively). Both USGS stations are co-located with Louisiana Coastal Protection and Restoration Authority System-wide Assessment Monitoring Program stations. One bottom-mounted upward-facing 1000 kHz Teledyne Sentinel V Acoustic Doppler Current Profiler (ADCP) and one RBRduet<sup>3</sup> channel logger were deployed at each station on a flat bed. ADCPs were programmed to collect 1024 samples at a sampling rate of 2 Hz on 120-min intervals. The ADCPs collected horizontal east-west (u), north-south (v), and vertical (w) current velocities at either 0.3 m or 0.35 m depth cells. ADCPs additionally recorded water level and wave parameters including significant wave height  $(H_s)$ , peak wave period  $(T_n)$ , and directional spectra of wave propagation  $(D_n)$ . RBRs recorded pressure variation on a 2 Hz basis to calculate the depth of the water column, and Ruskin software utilized linear wave theory to calculate  $H_s$ ,  $T_p$ , and water level. The instruments were deployed with self-contained settings between August 3 and September 25, 2020, and real-time settings between June 15 and August 23, 2021. The ADCP located at BBS failed in 2020, thus no data was recovered from that instrument for the 2020 deployment. The 2021 deployment period was cut short when Hurricane Ida made landfall near Barataria Bay on August 29, 2021, destroying both measurement stations and resulting in a loss of data collected after the final data transfer on August 23, 2022.

Concurrent wind speed and directional data were obtained from several locations within Barataria Bay, including the USGS Barataria Bay station 07380251 (BBN), NOAA station 8761724, and USGS Station 073802516 located at Barataria Pass adjacent to Grand Isle (used for the BBS station). Wind speeds were recorded in 30-min intervals at 10 m above sea level (m asl) at BBN and 20 m asl at BBS. Using the methods outlined in Mariotti et al. (2018), wind speeds from BBS were corrected to 10 m. The meteorological data from the NOAA station were used determine representative wind conditions throughout 2020–2021. During the 2021 deployments, wind data were only available through July 26, 2021 due to instrument failure associated with Hurricane Ida.

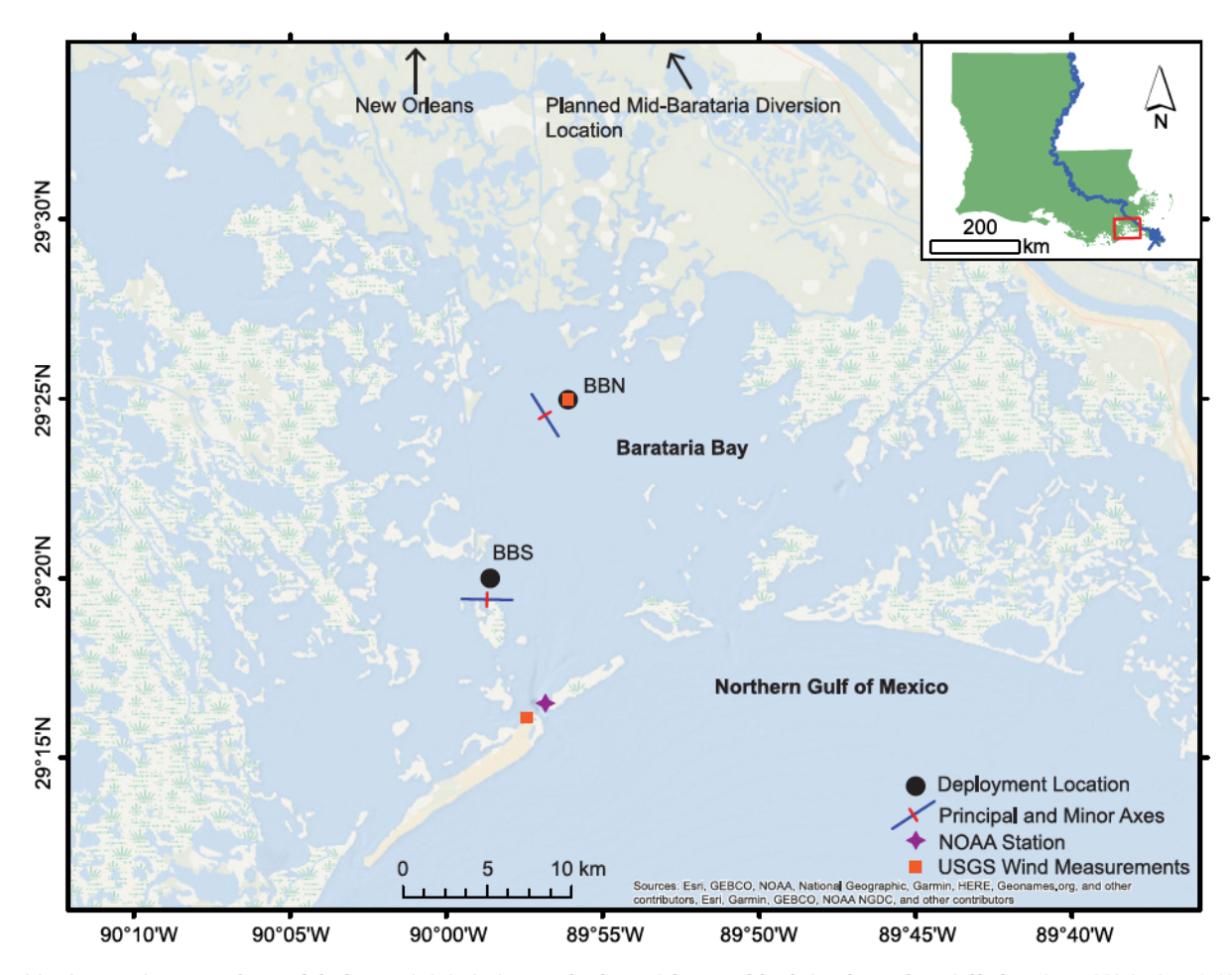


Fig. 1. Louisiana's Barataria Bay, southwest of the lower Mississippi River, south of New Orleans, and bordering the northern Gulf of Mexico. USGS Stations 07380251 and 073802514 are labeled BBN (Barataria Bay North) and BBS (Barataria Bay South) where upward-facing ADCPs and wave recorders were placed to measure wave and current activity. USGS Station 07802516 and NOAA Station 8761724 are located to the south of the measurement stations. The principal (blue) and minor (red) axes of mean current direction at each site are displayed adjacent to the site markers. The basemap is from ArcGIS online.

#### 2.3. Data analysis

ADCPs measured water velocity at each bin of 0.3 m (2020) to 0.35 m (2021). To identify the dominant flow direction, velocity data were rotated to principal and minor axes using principal component analysis, with principal and minor axes at BBN as 325° and 235°, relative to true north (from 2020 data), and 273° and 93°, respectively, at BBS. To characterize residual current variation during the deployments, velocities were filtered using a sixth-order low-pass Butterworth filter, with a cutoff frequency of 40 h (Butterworth et al., 1930; Li et al., 2019). To disentangle contributions from astronomical and meteorological sources to the observed periodicity of currents, a Fast Fourier Transform was used to isolate dominant frequencies in the velocity time series. Tidal constituents were identified as diurnal (0.8-1.1 cycles day<sup>-1</sup>), intertidal (1.1-1.8 cycles day<sup>-1</sup>), semidiurnal (1.8-2.2 cycles day-1), and overtidal (2.2-8.0 cycles day-1) based on previous analyses of tidal constituents at a southern Barataria Bay inlet (Li et al., 2019). Constituents with lower frequencies than 0.8 cycles day-1 to one cycle every 14 days were considered subtidal. Individual bands were normalized by the respective frequency range, to gauge the relative contribution of each frequency band to the overall signal. Analyses were conducted on the depth-averaged velocities.

A depth-attenuation correction was implemented on pressure data based on frequency. Corrected wave data were compared to a semi-empirical model created by Young and Verhagen (1996) to assess wave generation. The model uses inputs of varying or averaged water depth, wind speed, and fetch to calculate expected Hs. Wave periods were calculated to complement this analysis.

The mean tidal and subtidal directions of DACs were quantified for several different time periods: throughout the whole deployment, during storm events, and in quiescent periods (between storms). Given the shallow nature of the bay, vertical velocities are small and therefore not included in the analysis. Recorded velocities during each storm event were divided into two periods of pre- and post-peak water level, with the intent of identifying similarities or differences in recorded DAC magnitude and directionality for each storm. The duration obtained for the pre- and post-peak water level was based on visual interpretation of sustained disruption to the tidal and subtidal water level and tended to land within one to three days before and after the landfall of each storm event.

## 3. Results

## 3.1. Wind climate and water level

During the 2020 and 2021 deployments, four named TCs impacted Barataria Bay: Hurricane Laura (Laura), Hurricane Sally (Sally), Tropical Storm Beta (TS Beta), and Tropical Storm Claudette (TS Claudette). Hurricane propagation paths are provided in Fig. 2. Laura made landfall at 0600 UTC on August 27, 2020, approximately 330 km west of Barataria Bay in Cameron, Louisiana, with a forward propagation speed of 7–8 m s<sup>-1</sup> (Pasch et al., 2021). Sally made landfall at 0945 UTC on September 16, 2020, approximately 250 km to the east in Baldwin County, Alabama, moving slowly at <1 m s<sup>-1</sup> (Berg and Reinhart, 2021). TS Beta made landfall at 0245 UTC on September 22, 2020,

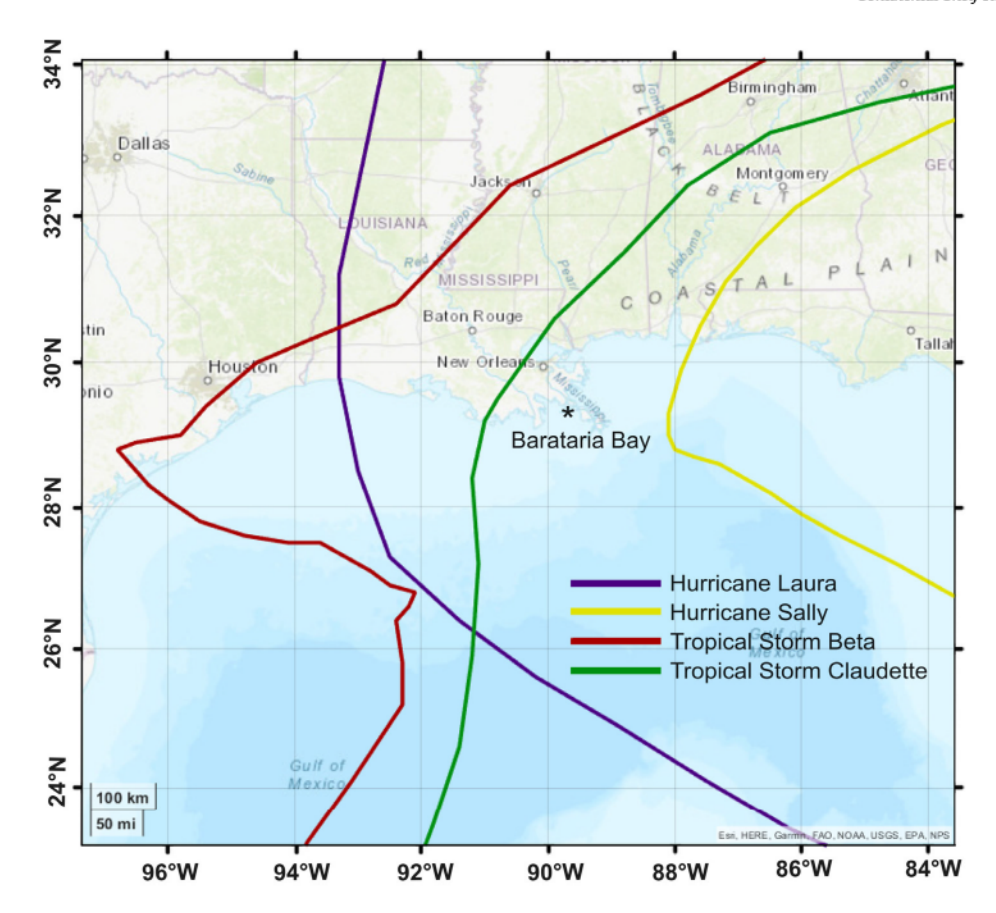


Fig. 2. Tracks of Hurricanes Laura and Sally (2020), and Tropical Storms Beta and Claudette (2020 and 2021, respectively). Data acquired from NOAA (2022).

approximately 670 km southwest of Barataria Bay in Matagorda Bay, Texas, with a propagation speed of 3 m s $^{-1}$  (NOAA, 2022). The one measured storm in 2021, TS Claudette, made landfall at 0430 UTC on June 16, 2021, in Terrebonne Parish, Louisiana, approximately 110 km southwest of the bay, moving at 2 m s $^{-1}$  (Papin and Berg, 2022; NOAA, 2022). Landfall times were used to isolate the effects of each event on waves and currents within the bay.

Wind speeds recorded within the bay during 2020 and 2021 rarely exceeded 10 m s $^{-1}$ , with the exception of the four notable storm events (Fig. 3), and the majority of the time wind speeds are less than 5m s $^{-1}$  blowing from primarily the SE and NW. Maximum wind speeds at BBN during the 2020 deployment reached 15.3 m s $^{-1}$ , while speeds up to 22.5 m s $^{-1}$  were recorded at Grand Isle near BBS, both measured during the passage of TS Beta (Fig. 3). Similarly, maximum wind speeds during the 2021 deployment were recorded at 16.9 m s $^{-1}$  during TS Claudette. Across both stations, average wind directions during Laura, Sally, and TS Beta were 177°, 11°, and 77° relative to true north, respectively, and 184° during TS Claudette.

The water depth during the 2020 deployment averaged 2.78 m at BBN and 2.27 m at BBS, with maximum depths reaching 3.62 m at BBN during Laura and 3.06 m at BBS during TS Beta. During the 2021 deployment, water depths averaged at 2.95 m and 2.13 m at BBN and BBS, respectively, with depths reaching a maximum of 3.43 m (BBN) and 2.55 m (BBS) during the passage of TS Claudette (Fig. 4). In general, the passage of a TC was marked by a rapid surge in water levels, followed by a decrease in water levels comparable to those measured during quiescent periods. A notable exception to this trend was observed during Sally, in which tidal and subtidal water levels appeared minimally affected compared to measurements during Laura, TS Beta, and TS Claudette. During quiescent periods, subtidal water levels fluctuated only slightly without the influence of TCs. The maximum tidal range at BBN reached 0.64 m and 0.61 m at BBS, both occurring during a tropical tidal cycle in 2021.

### 3.2. Current regime

### 3.2.1. Current velocity

Current velocities obtained from ADCPs during the 2020 (BBN) and 2021 (BBN and BBS) deployments were assessed. North-south and east-west velocity data were rotated to the axis of greatest variance (principal axis) and least variance (minor axis) (Fig. 1). Along the principal and minor axes at both stations, a signature diurnal ebb and flood current was observed at all recorded depths, and velocities were enhanced during tropical tides and diminished during equatorial tides (Fig. 5b and c). Current velocities observed within the upper 10%-15% of the water column appear to occasionally depart from this trend during times when overlying winds are moving in a sustained direction. In periods where wind direction is maintained, surface tidal currents follow the direction of wind propagation (Figs. 5, 6, 7). This correlation between wind and current direction did not appear to influence the central and lower portions of the water column. The relationship between wind and near-surface currents is most evident during the passage of Sally, though the correlation was also observed during several quiescent periods in 2021, including June 26-28 and July 3-5, in which surface currents opposed ebb and flood velocities that marked central and lower portions of the water column (Fig. 6 post-Claudette).

Current velocity data were processed to analyze subtidal velocities at BBN and BBS (Figs. 5d-e, 6d-e, 7d-e). At BBN, subtidal current magnitude and direction rarely diverged from mean observations, and this deviation occurred as expected during storm activity. BBS, however, is characterized by strong subtidal movement along the principal axis (273°) regardless of storm conditions, and subtidal current magnitudes at BBS tend to be stronger than similar measurements at BBN (Figs. 6 and 7). Similar to unfiltered currents, a noticeable correlation between wind and current directionality appeared in the subtidal signal.

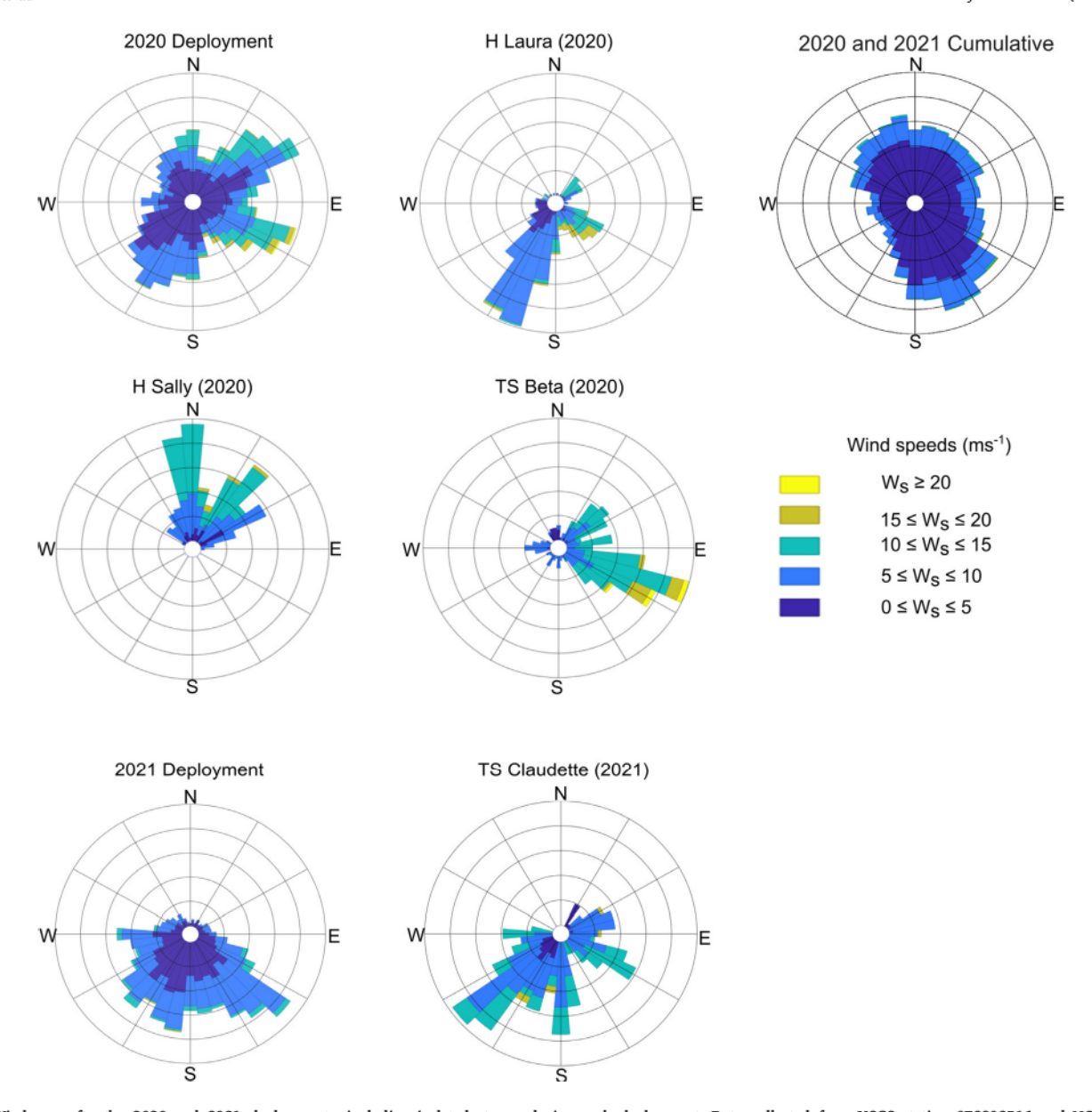


Fig. 3. Wind roses for the 2020 and 2021 deployments, including isolated storms during each deployment. Data collected from USGS station 073802516 and NOAA station 8761724 (cumulative), at Barataria Pass.

Table 1

Pre- and post-peak water level mean direction and magnitude of DAC velocity during the passage of four storms in 2020 and 2021. All values are given for BBN unless specified otherwise. Directions are given as the angle from which the currents are moving.

Event	Pre-peak water level mean velocity (m s <sup>-1</sup> )	Post-peak water level mean velocity (m s <sup>-1</sup> )	Pre-peak water level mean direction (° from N)	Post-peak water level mean direction (° from N)
Hurricane Laura	0.13	0.11	142	288
Hurricane Sally	0.01	0.06	157	286
TS Beta	0.05	0.09	146	51
TS Claudette	0.09	0.05	107	299
TS Claudette (BBS)	0.15	0.13	80	245

Recorded storms that made landfall to the west of the bay, especially those dominated by winds from the south prior to landfall (Laura and TS Claudette), showed strong storm surge along the principal axis followed by a sharp transition to ebb-dominated flow (Fig. 2). In contrast, Sally, which made landfall to the east of the bay, was characterized by winds from the north and displayed a relatively minimal subtidal surge, followed by relatively minimal observed subtidal ebb post-landfall (Fig. 5d–e).

#### 3.2.2. Depth-averaged velocity

Mean depth-averaged current (DAC) magnitudes and directions were calculated for pre- and post-peak water level time periods during each storm in order to gain insight into the differing hydrodynamic responses to meteorologic conditions (Table 1). Results indicate DAC velocities are dominated by expected diurnal, tropical, and equatorial tidal oscillations (Fig. 8). During the quiescent period of 2020 at BBN, mean DAC horizontal velocities were 0.09 m s<sup>-1</sup> with a net direction of

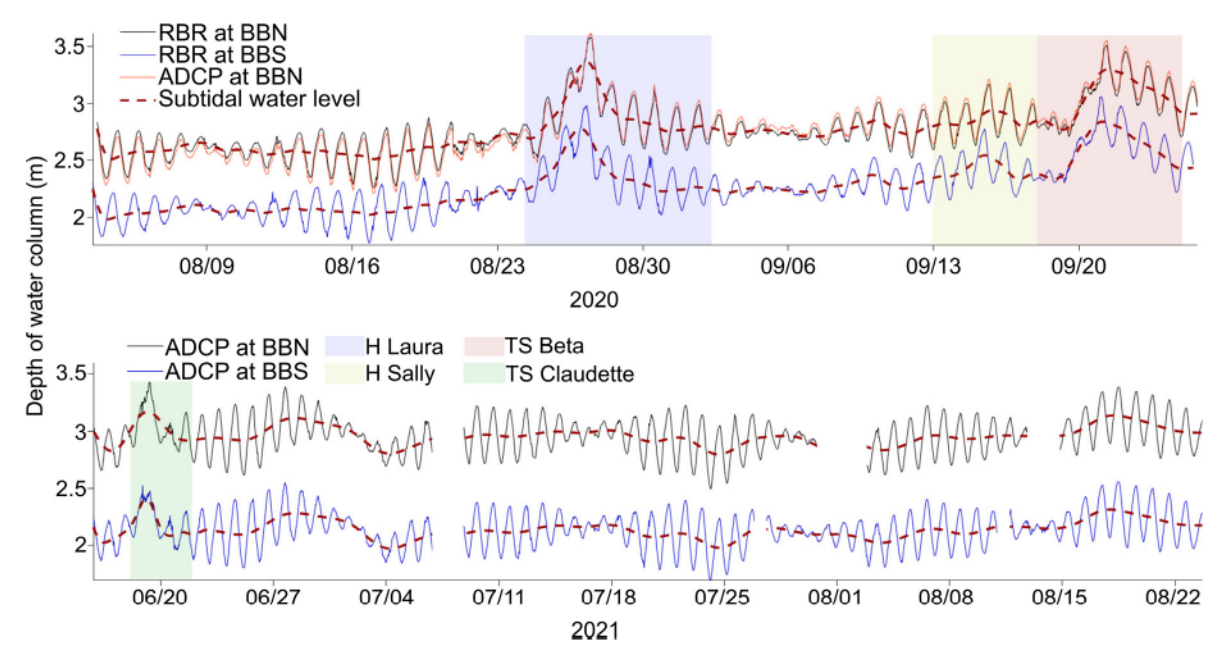


Fig. 4. Water depth (m) measurements during the 2020 and 2021 deployments at BBN and BBS. Data gaps represent signal connectivity issues during real-time data transfers.

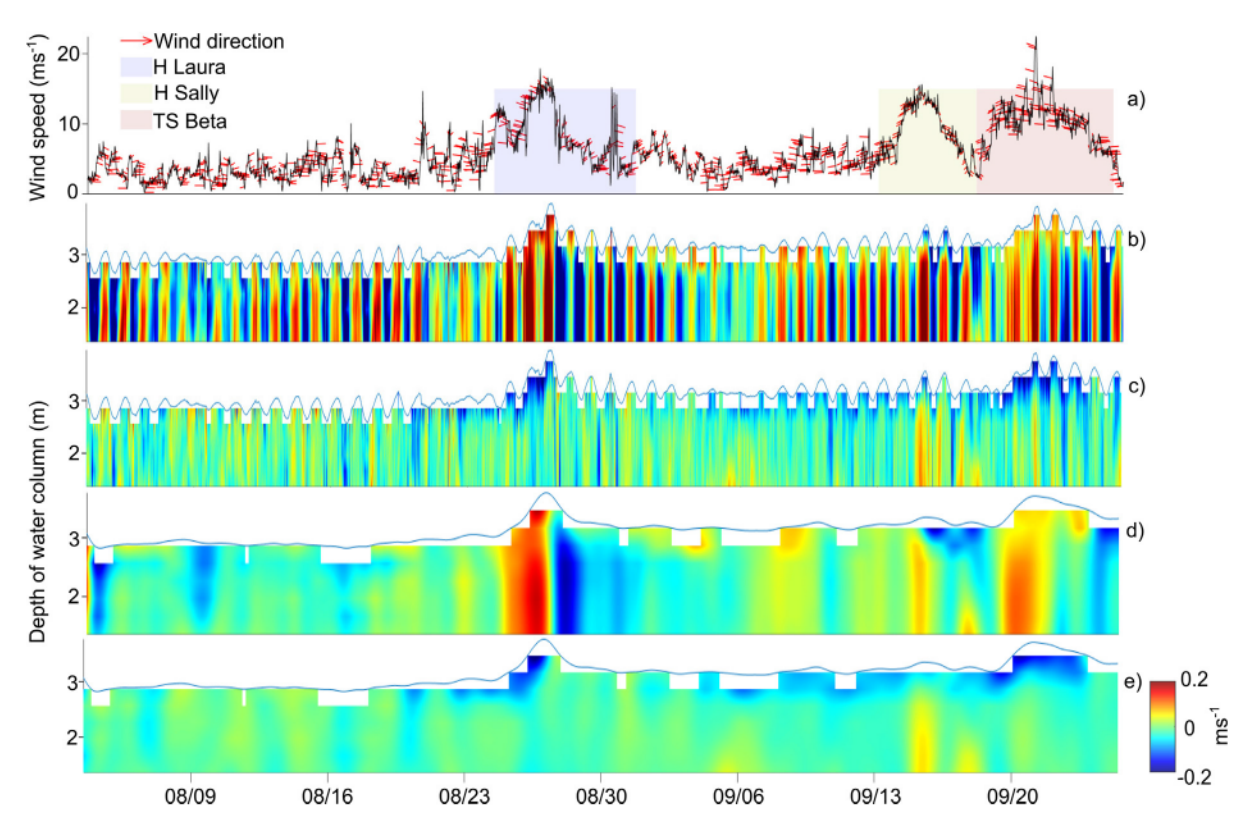


Fig. 5. ADCP measurements at BBN during the 2020 deployment. Wind direction and magnitude (a). Measured tidal currents along the positive principal axis (325°) and positive minor axis (235°) (b, c). Subtidal current measurements along both the principal and minor axes (d, e).

 $32^{\circ}$  relative to true north. Mean DAC horizontal velocities reached 0.05 m s<sup>-1</sup> with a net direction of  $22^{\circ}$  relative to true north. It should be noted that similar to the analysis of wind measurements, water velocity is given as the direction from which the water is moving, rather than to. Maximum velocities during the entirety of the 2020 BBN deployment reached 0.43 m s<sup>-1</sup> with a direction of  $321^{\circ}$ , which occurred during

the passage of Laura and 0.38 m s $^{-1}$  with a direction of 126° during TS Claudette. BBS captured a maximum velocity of 0.64 m s $^{-1}$  and direction of 105° during TS Claudette.

It is important to recognize the differences in DAC velocities and directions with respect to each storm, as each storm had a unique signature on DAC velocities and directions at both BBN and BBS. All four

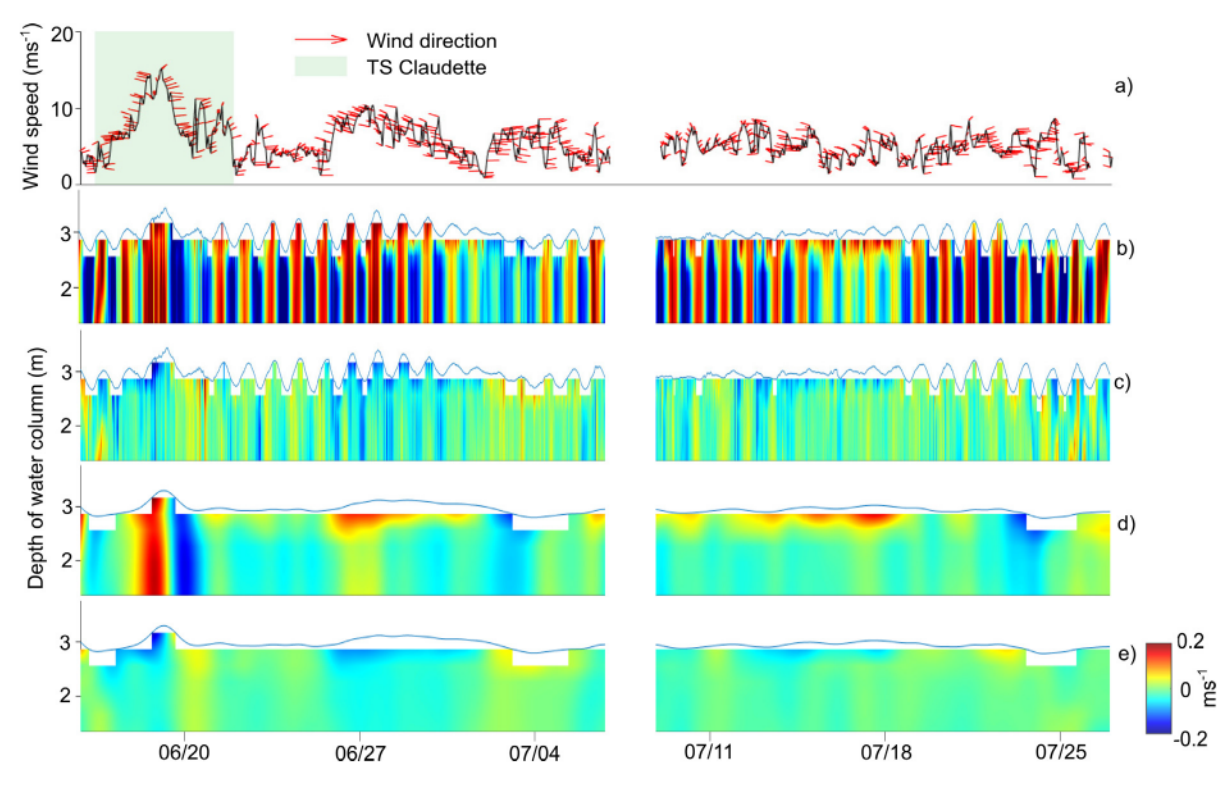


Fig. 6. ADCP measurements at BBN during the 2021 deployment. Wind direction and magnitude (a). Measured tidal currents along the principal and minor axes (b, c). Subtidal current measurements along the principal and minor axes (d, e). Due to damages to the station, wind data after approximately July 25, 2021, were unavailable.

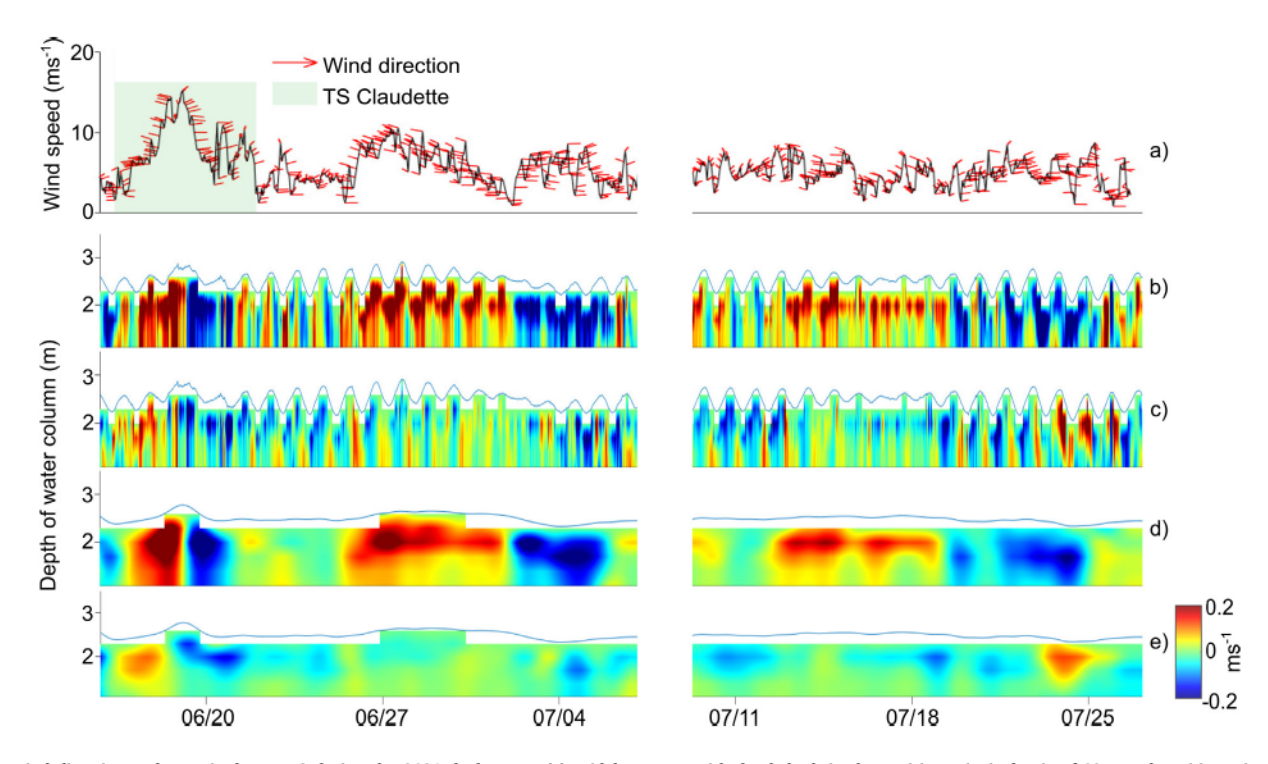


Fig. 7. Wind direction and magnitude at BBS during the 2021 deployment (a). Tidal currents with depth both in the positive principal axis of 325° and positive minor axis of 55° (b, c). Subtidal current directions in both the principal and minor axes (d, e). Due to damages to the station resulting from Hurricane Ida, wind data after approximately July 25, 2021, were unavailable.

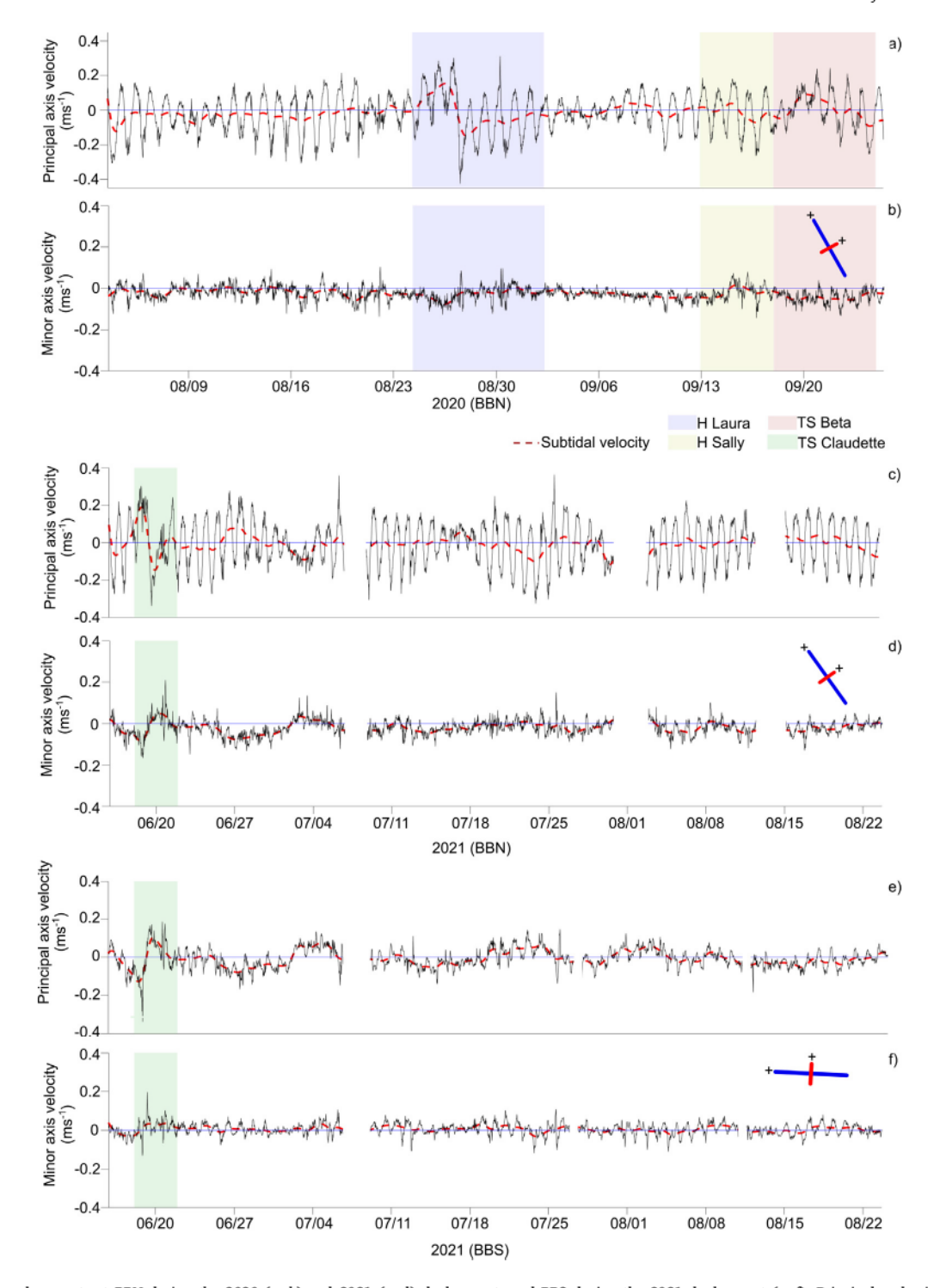


Fig. 8. Depth-averaged currents at BBN during the 2020 (a, b) and 2021 (c, d) deployments and BBS during the 2021 deployment (e, f). Principal and minor axes at BBN are 325° and 235°, relative to true north, while BBS is 273° and 3°, respectively.

recorded storms at BBN recorded DAC directions that were predominantly southeasterly before peak water level was reached (pre-peak) (Table 1). Post-peak DAC directions for the three storms that made landfall to the west of BBN were predominantly west-northwesterly, while TS Beta recorded northeasterly post-peak DAC direction. BBN post-peak DAC mean magnitudes were comparable to those experienced in pre-peak conditions during Laura, while those measured during Sally, which made landfall to the east of the bay, displayed post-peak mean magnitudes more than 5 times that experienced during pre-peak, which was notably low, at a recorded 0.01 m s<sup>-1</sup>. Beta showed post-peak magnitudes nearly double that of pre-peak, while

pre-peak magnitudes during Claudette were nearly double that of those measured during post-peak (Fig. 5a-b).

BBS recorded DACs during one storm (TS-Claudette) in 2021. Prepeak DAC direction was recorded as east-northeasterly, followed by a post-peak southwesterly direction. DAC mean magnitudes at BBS during TS Claudette were larger than those measured during other notable storms in 2020 and 2021 at BBN (Table 1).

Depth-averaged subtidal flow at BBN appeared to be most affected by Laura along the principal axis during the 2020 deployment, while Sally disrupted flow significantly less so than both Laura and TS Beta, though local wind speeds for each event were comparable in magnitude. Visual analysis of subtidal DAC velocity additionally reveals a predominant flow from the northeast at BBN and a slight flow from the south at BBS during quiescent periods (Fig. 8). During the initial disruption caused by Laura, DAC velocities changed to a strong southeasterly direction, and magnitudes were enhanced more than three times that of the recorded average during quiescent periods. After Laura made landfall, velocities reversed to a west-northwesterly direction, yet maintained magnitudes more than double that of quiescent periods. Sally, on the other hand, exhibited pre-peak DAC velocities weaker than those that were observed in quiescent periods, with an easterly directionality, while the post-peak currents moving to the south exhibited average magnitudes more than double those measured during pre-peak.

#### 3.2.3. Spectral analysis of currents

A Fast Fourier Transform (FFT) was conducted on depth-averaged currents with the goal of assessing how a storm disrupts the relative distribution of energy across frequency ranges associated with tidal constituents (Fig. 9). FFT analysis reveals strong  $O_1$  (25.84 h) and  $K_1$ (23.93 h) tidal components and, to a lesser extent,  $M_2$  (12.42 h) and  $S_2$ (12.0 h) components. As expected, FFT results at BBN during quiescent periods in 2020 and 2021 show the highest relative power associated with the diurnal constituent, which represents more than 50% of the total relative energy within the system, followed by subtidal, semidiurnal, intertidal, and finally overtidal constituents (Fig. 9). Both Laura and Sally made landfall during a tropical tidal cycle, while TS Beta and TS Claudette made landfall during an equatorial tidal cycle. Regardless of landfall time, the relative power associated with the diurnal constituent diminished while that of the subtidal constituent was enhanced (Fig. 9). It appears for storms that made landfall during an equatorial tidal cycle, the relative contribution of the diurnal constituent decreases more substantially when compared to the relative diurnal contribution when a storm makes landfall during a tropical tidal cycle, as shown comparing Laura and Sally to Beta and Claudette at BBN (Fig. 9ad). Little change in overtidal, semidiurnal, and intertidal constituents occurs in the presence of a storm compared to quiescent periods.

The relative contributions of constituents to the overall signal were also compared between BBN and BBS stations. For consistency, when comparing tidal constituents between BBN and BBS, only the 2021 deployment is used, as disruption to the spectral signal takes place over the same period under similar meteorological conditions. At BBS, during quiescent periods, relative subtidal contribution to the overall signal is over 30%, while that of diurnal is slightly less than 30%. This is in contrast to a relative subtidal contribution of less than 25% and a relative diurnal contribution of over 50% at BBN during the 2020 and 2021 deployment periods. These results indicate that subtidal contribution to the overall signal is much stronger at BBS compared to BBN during quiescent periods. When TS Claudette made landfall, the relative diurnal contribution decreased across both stations, with a more significant decrease observed at BBN compared to BBS. The concurrent increase in subtidal relative contribution was observed to be more substantial at BBN compared to BBS. The maximum contribution of the subtidal signal during TS Claudette increased to 70% at BBN and 90% at BBS (Fig. 9d-e).

### 3.3. Wave height

Average recorded Hs values during the 2020 deployment at BBN and BBS were 0.09 m and 0.13 m, respectively. Average Tp values recorded during Laura, Sally, and TS Beta were 2.85 s, 2.69 s, and 2.92 s, respectively. No wave information was able to be processed for the quiescent period of 2020 due to the magnitude of pressure attenuation affecting RBR measurements and backscatter affecting ADCP measurements. Wave information was also unable to be obtained during the 2021 deployment at BBN or BBS due to internal real-time wave processing errors.

Maximum recorded Hs during Laura, Sally, and TS Beta reached 0.83 m, 0.38 m, and 0.73 m at BBN, and 0.70 m, 0.38 m, and 0.91 m at BBS, respectively (Fig. 10). Maximum Tp during Laura, Sally, and TS Beta was 3.43 s, 3.09 s, and 3.51 s at BBN, and 3.32 s, 3.21 s, and 3.66 s at BBS, respectively. The maximum Tp of 3.66 s (TS Beta) suggests waves within the bay are primarily locally-generated, even during the passage of TCs. The duration of sustained heightened Hs during TS Beta appears to last longer when compared to the observed rapid decrease in Hs after Laura made landfall and relatively low Hs measured during Sally (Fig. 10).

Wave propagation directions for Laura, Sally, and TS Beta were recorded at  $157^{\circ}$ ,  $2^{\circ}$ , and  $120^{\circ}$ , respectively, while average wind directions for each storm reached  $171^{\circ}$ ,  $4^{\circ}$ , and  $61^{\circ}$ . The significant similarity in wave propagation direction and wind movement is evident during storms Laura and Sally, while TS Beta shows a  $59^{\circ}$  disparity.

A semi-empirical model for significant wave height (Young and Verhagen, 1996) with inputs of fetch, depth, and wind speed and output of Hs was run for the 2020 deployment. Results indicate a strong correlation between the model and measurements ( $R^2 = 0.77$ ; Fig. 10). When fetch, depth, and wind speed are known for the southern portion of Barataria Bay, Hs can be reasonably predicted using the semi-empirical model employed by Young and Verhagen (1996), even during isolated storm events, such as Laura ( $R^2 = 0.77$ ), Sally ( $R^2 = 0.69$ ), and Beta ( $R^2 = 0.68$ ) (Fig. 10).

#### 4. Discussion

#### 4.1. The effect of storms on water levels

Observed wind speeds in Barataria Bay were remarkably similar during all four storm events recorded during the 2020 and 2021 deployment periods (Figs. 5 and 6(a)). Laura, Sally, and TS Claudette maintained increased wind speeds for a similar duration, while speeds during TS Beta decreased at a comparably slower rate following landfall, most likely due to the sustained northeastward propagation of TS Beta post-landfall. TS Beta immediately altered course to the east once landfall was made, increasing the duration of sustained high winds over Barataria. Subsequently, sustained elevated water levels were observed during and after TS Beta for a longer period of time compared to the other measured storms, which supports the notion that the post-landfall track of a tropical storm can affect the duration of elevated water levels.

The relatively large increase in water level during all events except Sally is most likely due to the cyclonic nature of storms within the GoM (Paron, 2014). As Sally made landfall to the east of the observation stations, sustained local winds were from the north, resulting in decreased water levels (Fig. 4). The timing of landfall for each storm had additional effects on water levels. Due to the low tidal range associated with equatorial tide in the nGoM, wind-driven hydrodynamics resulting from TS Claudette, which made landfall during an equatorial tide, dominated water level variation, as the contribution of diurnal tides to overall change in water level was diminished (Fig. 4). As Laura made landfall, however, the enhanced diurnal tidal range of a tropical tidal cycle resulted in higher peak water levels brought about by the storm. Though recent research suggests storm propagation speed plays a primary role in controlling surge along the Louisiana coast (Musinguzi and Akbar, 2021), results from this study suggest the correlation between propagation speed of a storm and heightened water levels is less pronounced than models would suggest, at least within a barrier-island protected system like Barataria Bay. It appears that sustained winds from the south are the main driver of enhanced water levels, coupled with the phase of the underlying tidal cycle (Fig. 4). As storms that make landfall to the west of the bay are more likely to be characterized by sustained winds from the south, these storms are more likely to drive increased surge within the bay, especially if landfall occurs during a peak tropical tidal cycle (Chen et al., 2008). Based on these observations, the direction of sustained winds and the timing of tropical and

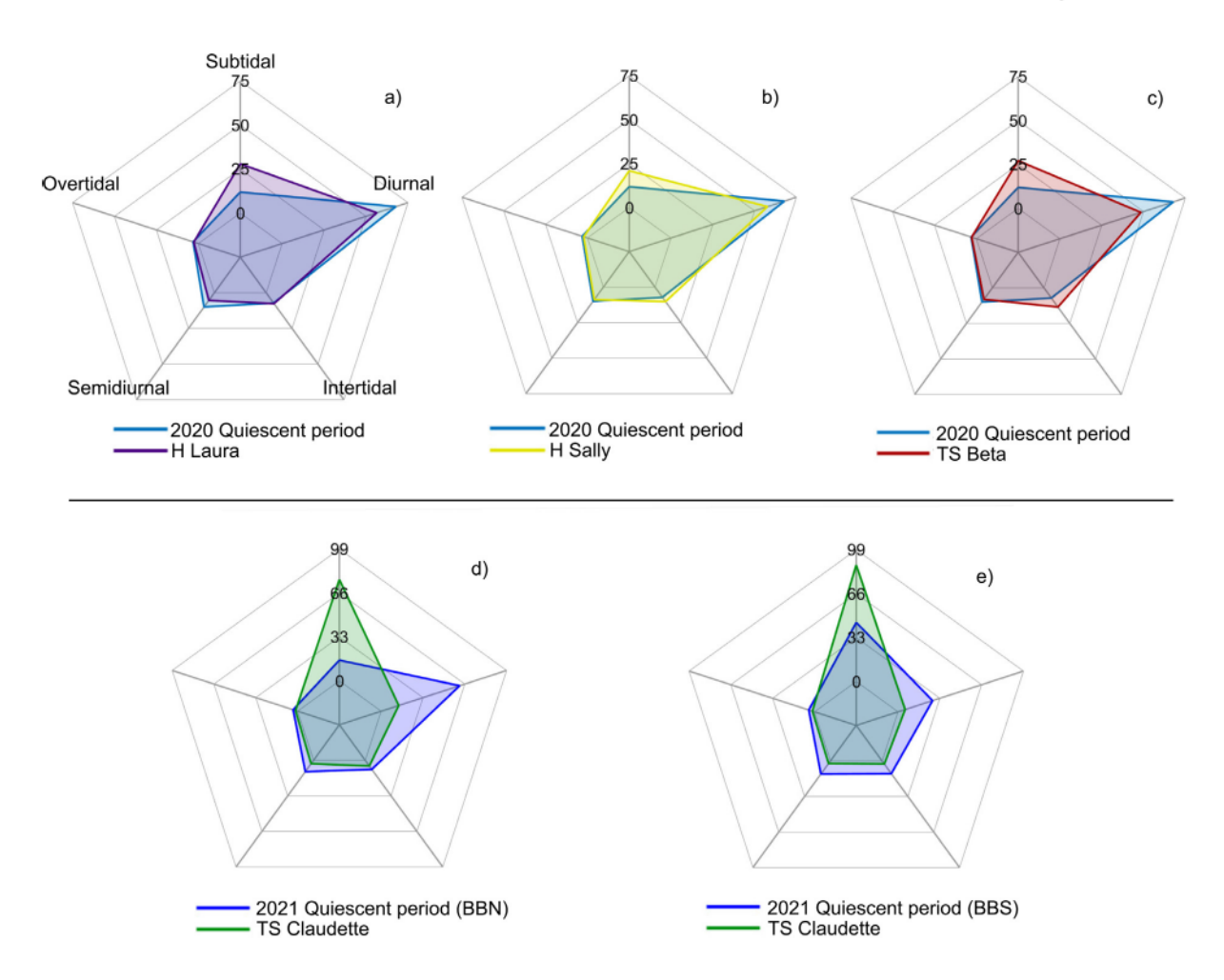


Fig. 9. Relative power as a percentage associated with each tidal constituent of the depth-averaged velocity during the quiescent periods of 2020 and 2021 compared to the four storm events during the deployments (a, Laura at BBN; b, Sally at BBN; c, Beta at BBN; d, Claudette at BBN; e, Claudette at BBS).

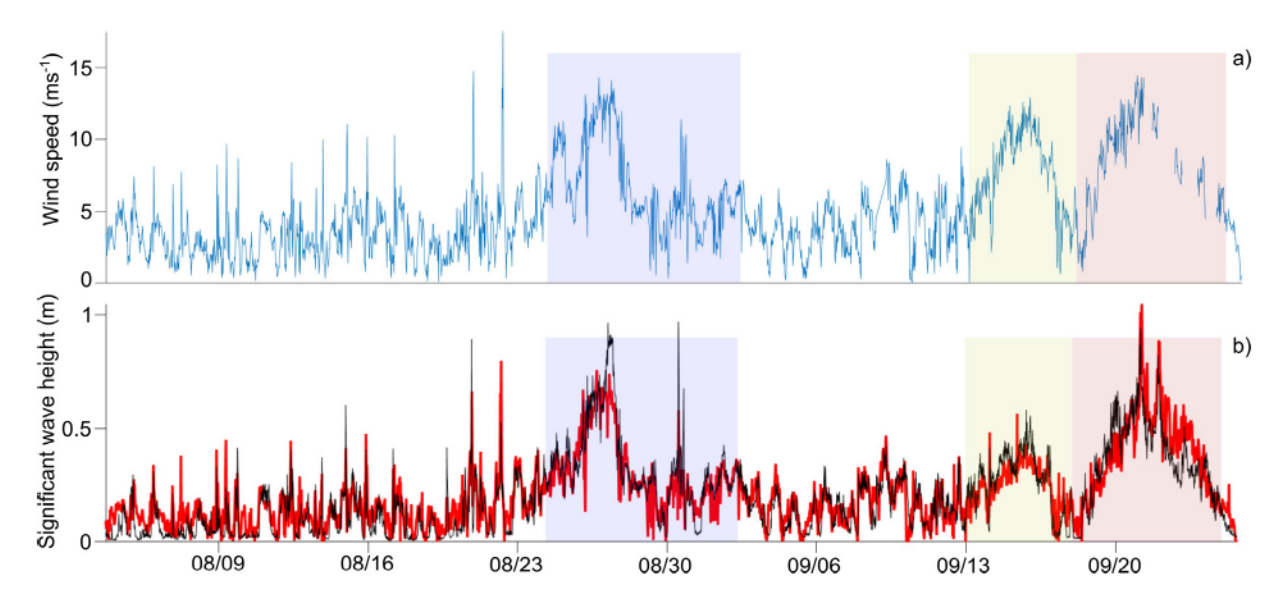


Fig. 10. Wind speed measured at BBN during the 2020 deployment (a). Wave climate, both modeled (red) and measured (black).

equatorial tidal cycles are, as expected, the dominant factors affecting water levels when a storm impacts Barataria Bay. Future observational research on the impact of sustained winds and other parameters such as location of storm landfall and storm propagation speed on water level variation is needed to inform predictive numerical models and mitigate flood impacts (Shashank et al., 2021; Bilskie et al., 2016; Vijayan et al., 2021). Future studies might incorporate an increased number of measurements spatially and temporally throughout Barataria Bay. In addition, rainfall measurements will increase our understanding of meteorological contributions to water level variability.

#### 4.2. Current regime

Depth-averaged currents (DACs) during each measured storm event reveal the non-uniform effect storms have on disrupting the direction and magnitude of currents within Barataria Bay. The unique signatures of DAC directions and magnitudes resulting from observed storms speaks to the complexity of nearshore hydrodynamic systems, especially when subject to meteorologic events. Similar hydrodynamic responses were expected from all three storms that made landfall to the west of the bay, however, the northeasterly post-peak mean directionality of DACs during TS Beta (BBN), and east-southeasterly pre-peak measurements during TS Claudette (BBS) revealed this was not the case. Pre- and post-peak DAC mean magnitudes were comparable at BBN for only Laura (Fig. 8). The post-peak mean DAC magnitude experienced during Beta was nearly twice that measured during the prepeak surge. The opposite was observed for Claudette, indicating each storm has a unique perturbation to underlying currents within Barataria Bay, at least within the general area of BBN. In all cases, velocities return to normal very quickly following the passage of a TC, and there appears to be no cumulative affect on currents due to the sequential nature of the storms (e.g., Sally and Beta). Furthermore, the relatively strong southern moving current post-peak during Sally, compared to a weak pre-peak DAC magnitude, provides evidence that relatively diminished storm surge and following enhanced seaward flow is likely to occur after a storm makes landfall to the east of the bay (Chen et al., 2008). This supports previous findings that net nearshore current responses to the west of a cyclonic storm will be ebb dominant and result in a net outward flow of water, with implications for net seaward transport of sediment (Goff et al., 2019). Sediment deposition may be enhanced during periods of sustained winds from the south (Li et al., 2021), because of the velocity reduction imposed by wind stress, which carries important implications for the operations of controlled sediment diversion proposed in the region aimed at building land.

Both tidal and subtidal flow throughout the entirety of the water column was expected to be dominated by storm surge and move in a similar direction regardless of the observed storm, due to the limited tidal forcing in the nGOM. This was not the case, however, as during storms such as Sally and Beta, flow follows expected surge directions within the central portions of the water column while the top portion of the water column appears to follow the direction of overlying sustained winds (Fig. 5). This effect has previously been described as windinduced surface currents (Ren et al., 2015) and can inform mixing processes in shallow bays during storms. Further research needs to be conducted to delineate the depth within the water column where the effects of local wind diminish when compared to tidal forcing and storm surge, which may give insight into the movement of water and entrained material or dissolved constituents in the upper portions of the water column during TCs.

Nearshore currents in proximity to subaerial marsh platforms are strongly influenced by the complex geometry of Barataria Bay. For example, the preferential flow of currents along the principal axis at BBS, which is nearly in direct east—west orientation, is only magnified during the passage of Claudette (Fig. 7). Though Claudette was defined by winds from the south and propagated to the north as it made landfall, current velocities, both depth-averaged and throughout the

entire water column at BBS are in predominately east—west directions. As shown in Fig. 1, Mendicant Island (north) and an unnamed marsh platform (south) act to direct water in both calm periods where daily tides characterize water movement and during the passage of storms. Additional research is needed to characterize the effect of subaerial platforms of varying geometries and sizes in channelizing flow on the fringes of open bay systems, and how the rapid degradation and disappearance of such platforms in coastal Louisiana (Barras et al., 2003) will alter current regimes in the future. Predicting impacts on current velocities may inform decision-makers on where to concentrate restoration efforts.

Spectral analysis of depth-averaged currents demonstrates that all storms had the effect of diminishing the relative influence of diurnal contributions to the power of the signal, while subtidal contributions were enhanced (Fig. 9). This was especially visible during Beta and Claudette and can most likely be attributed to the fact that both storms made landfall during an equatorial tidal cycle, resulting in a comparably diminished magnitude of the diurnal signal compared to Laura and Sally. This means that as a storm passes during an equatorial tide, subtidal contributions to the signal are being compared to relatively diminished contributions of diurnal signals, and thus, appear to be disproportionately magnified. If a storm makes landfall during an equatorial tide, for example, the subtidal direction of currents may provide insight into residence times and flushing rates of introduced water. For example, Defne and Ganju (2015) found that local winds inducing subtidal motion during meteorologic events in a back-barrier bay can reduce residence times substantially.

#### 4.3. Wave height

Though wind magnitudes were relatively similar across all three storm events in 2020, wave heights varied significantly (Fig. 10). At BBN and BBS, Hs appears to gradually increase before drastically decreasing as a result of Laura, and Hs reached heights nearly double that of Sally during Laura. Hs during Beta, on the other hand, increased more dramatically followed by a gradual decrease. This would indicate that though there may be a disparity in wave heights between each event, wave direction, as expected, is largely influenced by overlying wind speed and sustained directionality, as was observed during Laura and Sally in 2020 and in previous analyses (Valentine and Mariotti, 2019). This may be attributed to the sustained high wind intensity coupled with the long fetch that marked Beta, while Laura's fast propagation speed resulted in a rapid decline of wind intensity following landfall. Alternatively, Sally was marked by winds moving to the south, with diminished fetch compared to both Laura and Beta (Fig. 3).

Analysis of Tp indicates that the recorded waves are locally generated, as during each storm event Tp did not reach more than 3.66 s, providing evidence of the role that barrier islands have in attenuating swell as water enters the bay during a storm, resulting in waves that are influenced predominantly by local winds. When the Mid-Barataria Diversion Structure is implemented, introduced suspended sediment and nutrients will most likely be influenced by overlying wind waves compared to the influence of currents and thus sediments will most likely be subject to resuspension via locally-generated waves, though the measured impact of hydrodynamics on potential resuspension is outside the scope of this study. The compounding effects of barrier islands on the southern border of the bay as well as the shallow depth contribute to limiting the magnitude of wave heights within the bay (Cobell et al., 2013). However, it is likely that feedbacks among high rates of relative sea level rise, wetland loss, increasing tidal prism, and widening of barrier island tidal inlets (FitzGerald et al., 2007, 2008; Kindinger et al., 2013, 2015; Hiatt et al., 2019), even with the competing effects of coastal protection and restoration strategies, may lead to increased wave heights and swell influence in Barataria Bay. Given the significant erosion of barrier islands protecting Barataria Bay (Kindinger et al., 2013), projections of future wave climate are of utmost importance for the resiliency of wetland complexes within the region and the landforms generated by large-scale sediment diversions like the Mid-Barataria Diversion. Thus, the region serves as a case study for understanding the competing effects of relative sea level rise and engineered coastal protection efforts that are predicted to affect deltaic systems worldwide (Day et al., 2007).

#### 5. Conclusions

In this study, current velocity and wave data were collected within Barataria Bay, Louisiana, in 2020 and 2021. The research captured the hydrodynamic response of four tropical cyclones and quantified the influence of storm landfall location, strength, directionality, and timing of associated winds, surrounding subaerial platform geometry, and storm surge. Major findings involving water levels, circulation, and waves are: (1) Water levels and depth-averaged current velocities were observed to be uniquely modulated by the location and concurrent wind speed of each passing storm. Storms making landfall to the west of the system enhanced subtidal velocities while the one recorded storm that made landfall to the east had a limited effect on surge. (2) During tropical cyclones, currents within the upper portion of the water column appear be dominated by local winds while the central and lower portions of the water column were observed to be modulated by storm surge in generally northwest to southeast directions. (3) The complex geometry of the fragmented subaerial marsh platforms in the Barataria Bay system can direct flow both during quiescent periods and during the passage of a storm. (4) Waves within Barataria Bay are generated by local prevailing winds and can be predicted using a semiempirical model with inputs of fetch, water depth, and wind speed. (5) Storm events have a unique signature on sub-tidal current velocities, depending on storm track and time of impact relative to the tidal cycle.

## CRediT authorship contribution statement

Jay Merrill: Writing – review & editing, Writing – original draft, Visualization, Validation, Methodology, Formal analysis, Data curation. Giulio Mariotti: Writing – review & editing, Investigation, Formal analysis. Chunyan Li: Writing – review & editing, Investigation, Funding acquisition. Matthew Hiatt: Writing – review & editing, Writing – original draft, Visualization, Supervision, Resources, Project administration, Methodology, Investigation, Funding acquisition, Conceptualization.

## Declaration of competing interest

The authors declare that they have no known competing financial interests or personal relationships that could have appeared to influence the work reported in this paper.

#### Data availability

https://doi.org/10.6084/m9.figshare.25050038.

## Acknowledgments

This work was supported by the Louisiana Coastal Protection and Restoration Authority (CPRA) through CPRA Task Order No. 4400017979/PO-2000468786. Any opinions, findings, and conclusions or recommendations expressed in this material are those of the author(s) and do not necessarily reflect the views of the CPRA. M.H. and C.L. also acknowledge funding through National Science Foundation Award 2023443. Special thanks is given to E. Weeks for logistical and field support. The authors acknowledge the contributions and vision of CPRA scientists, especially S. Khalil and R. Raynie. The authors thank the Associate Editor Ming Li, Phillip Orton, and one anonymous reviewer for constructive reviews.

#### References

- Allison, M.A., Sheremet, A., Goñi, M.A., Stone, G.W., 2005. Storm layer deposition on the Mississippi–Atchafalaya subaqueous delta generated by Hurricane Lili in 2002. Cont. Shelf Res. 25 (18), 2213–2232.
- Barras, J.A., Beville, S., Britsch, D., Hartley, S., Hawes, S., Johnston, J., Kemp, P., Kinler, Q., Martucci, A., Porthouse, J., et al., 2003. Historical and Projected Coastal Louisiana Land Changes: 1978-2050. United States Geological Survey, Reston, VA, IISA
- Berg, R., Reinhart, B., 2021. National Hurricane Center Tropical Cyclone Report: Hurricane Sally. Al 192020, National Oceanic and Atmospheric Administration, National Weather Service, Washington, DC.
- Bilskie, M.V., Hagen, S., Medeiros, S., Cox, A., Salisbury, M., Coggin, D., 2016. Data and numerical analysis of astronomic tides, wind-waves and Hurricane storm surge along the northern Gulf of Mexico. J. Geophys. Res.: Oceans 121 (5), 3625–3658.
- Bromirski, P.D., Kossin, J.P., 2008. Increasing Hurricane wave power along the US Atlantic and Gulf coasts. J. Geophys. Res.: Oceans 113 (C7).
- Butterworth, S., et al., 1930. On the theory of filter amplifiers. Wireless Eng. 7 (6), 536-541.
- Camelo, J., Mayo, T.L., Gutmann, E.D., 2020. Projected climate change impacts on hurricane storm surge inundation in the coastal United States. Front. Built Environ. 207
- Chen, Q., Wang, L., Tawes, R., 2008. Hydrodynamic response of northeastern Gulf of Mexico to Hurricanes. Estuar. Coasts 31 (6), 1098–1116.
- Cobell, Z., Zhao, H., Roberts, H.J., Clark, F.R., Zou, S., 2013. Surge and wave modeling for the Louisiana 2012 Coastal Master Plan. J. Coast. Res. (67 (10067)), 88–108.
- Couvillion, B.R., Barras, J.A., Steyer, G.D., Sleavin, W., Fischer, M., Beck, H., Trahan, N., Griffin, B., Heckman, D., 2011. Land area change in coastal Louisiana from 1932 to 2010.
- CPRA, 2023. Louisiana's Comprehensive Master Plan for a Sustainable Coast. Louisiana Coastal Protection and Restoration Authority.
- Day, J.W., Boesch, D.F., Clairain, E.J., Kemp, G.P., Laska, S.B., Mitsch, W.J., Orth, K., Mashriqui, H., Reed, D.J., Shabman, L., et al., 2007. Restoration of the Mississippi Delta: lessons from Hurricanes Katrina and Rita. Science 315 (5819), 1679–1684.
- Define, Z., Ganju, N.K., 2015. Quantifying the residence time and flushing characteristics of a shallow, back-barrier estuary: Application of hydrodynamic and particle tracking models. Estuar. Coasts 38 (5), 1719–1734.
- FitzGerald, D.M., Fenster, M.S., Argow, B.A., Buynevich, I.V., 2008. Coastal impacts due to sea-level rise. Annu. Rev. Earth Planet. Sci. 36, 601–647.
- FitzGerald, D., Kulp, M., Hughes, Z., Georgiou, I., Miner, M., Penland, S., Howes, N., 2007. Impacts of rising sea level to backbarrier wetlands, tidal inlets and barrier islands: Barataria coast, Louisiana. In: Coastal Sediments' 07. pp. 1179–1192.
- Georgiou, I.Y., FitzGerald, D.M., Stone, G.W., 2005. The impact of physical processes along the Louisiana coast. J. Coast. Res. 72–89.
- Goff, J.A., Swartz, J.M., Gulick, S.P., Dawson, C.N., de Alegria-Arzaburu, A.R., 2019.
  An outflow event on the left side of Hurricane Harvey: Erosion of barrier sand and seaward transport through aransas pass, Texas. Geomorphology 334, 44–57.
- Guerra-Chanis, G.E., So, S., Valle-Levinson, A., 2021. Effects of Hurricane Irma on residual flows and saltwater intrusion in a subtropical estuary. Reg. Stud. Mar. Sci. 41 (101), 568.
- Hiatt, M., Snedden, G., Day, J.W., Rohli, R.V., Nyman, J.A., Lane, R., Sharp, L.A., 2019. Drivers and impacts of water level fluctuations in the Mississippi River delta: Implications for delta restoration. Estuar. Coast. Shelf Sci. 224, 117–137.
- Holland, G., Done, J., Bruyere, C., Cooper, C.K., Suzuki, A., 2010. Model investigations of the effects of climate variability and change on future Gulf of Mexico tropical cyclone activity.
- Huang, W., Li, C., 2020. Contrasting hydrodynamic responses to atmospheric systems with different scales: Impact of cold fronts vs. that of a hurricane. J. Mar. Sci. Eng. 8 (12), 979.
- Hughes, J.E.T., 2016. A geochronological and stratigraphic reconstruction of the middle Barataria Bay receiving basin.
- Jankowski, K.L., Törnqvist, T.E., Fernandes, A.M., 2017. Vulnerability of Louisiana's coastal wetlands to present-day rates of relative sea-level rise. Nature Commun. 8
- Kindinger, J.L., Buster, N.A., Flocks, J.G., Bernier, J.C., Kulp, M.A., 2013. Louisiana Barrier Island Comprehensive Monitoring (BICM) Program Summary Report: Data and Analyses 2006 Through 2010. US Department of the Interior, US Geological Survey.
- Kindinger, J.L., Buster, N.A., Flocks, J.G., Bernier, J.C., Kulp, M.A., Miner, M.D., 2015. Impacts of relative sea-level rise and extreme storms on coastal geomorphic change and barrier island evolution in Louisiana. In: The Proceedings of the Coastal Sediments 2015. World Scientific.
- Kolker, A.S., Allison, M.A., Hameed, S., 2011. An evaluation of subsidence rates and sea-level variability in the northern Gulf of Mexico. Geophys. Res. Lett. 38 (21).
- LATIG, 2021. Mid-Barataria Sediment Diversion Draft Restoration Plan 3.2 and Environmental Impact Statement, Prepared by: Louisiana Trustee Implementation Group (LATIG), State of Louisiana, National Oceanic and Atmospheric Administration, US Department of the Interior, US Department of Agriculture, US Environmental Protection Agency.

- Li, C., Huang, W., Milan, B., 2019. Atmospheric cold front-induced exchange flows through a microtidal multi-inlet bay: Analysis using multiple horizontal ADCPs and FVCOM simulations. J. Atmos. Ocean. Technol. 36 (3), 443–472.
- Li, C., Weeks, E., Blanchard, B.W., 2010. Storm surge induced flux through multiple tidal passes of Lake Pontchartrain estuary during Hurricanes Gustav and Ike. Estuar. Coast. Shelf Sci. 87 (4), 517–525.
- Li, C., Weeks, E., Rego, J.L., 2009. In situ measurements of saltwater flux through tidal passes of Lake Pontchartrain estuary by Hurricanes Gustav and Ike in September 2008. Geophys. Res. Lett. 36 (19).
- Li, G., Xu, K., Xue, Z.G., Liu, H., Bentley, S.J., 2021. Hydrodynamics and sediment dynamics in Barataria Bay, Louisiana, USA. Estuar. Coast. Shelf Sci. 249 (107), 000
- Mariotti, G., Ceccherini, G., McDonell, M., Justić, D., 2022. A comprehensive assessment of sediment dynamics in the Barataria basin (LA, USA) distinguishes riverine advection from wave resuspension and identifies the Gulf Intracoastal Waterway as a major sediment source. Estuar. Coasts 45 (1), 78–95.
- Mariotti, G., Fagherazzi, S., Wiberg, P., McGlathery, K., Carniello, L., Defina, A., 2010. Influence of storm surges and sea level on shallow tidal basin erosive processes. J. Geophys. Res.: Oceans 115 (C11).
- Mariotti, G., Huang, H., Xue, Z., Li, B., Justic, D., Zang, Z., 2018. Biased wind measurements in estuarine waters. J. Geophys. Res.: Oceans 123 (5), 3577–3587.
- Miller, P.W., Trepanier, J.C., 2021. Predicting the Gulf of Mexico hurricane season with 500-hpa temperature. Geophys. Res. Lett. 48 (17), e2021GL094, 741.
- Muller, R.A., Stone, G.W., 2001. A climatology of tropical storm and hurricane strikes to enhance vulnerability prediction for the southeast US coast. J. Coast. Res. 949–956.
- Musinguzi, A., Akbar, M.K., 2021. Effect of varying wind intensity, forward speed and surface pressure on storm surges of Hurricane Rita. J. Mar. Sci. Eng. 9 (2), 128.
- NOAA, 2022. National oceanic and atmospheric administration (NOAA) National Hurricane Center. available online at <a href="http://nhc.noaa.gov/">http://nhc.noaa.gov/</a> (Accessed February 24 2022).
- Ortiz, A.C., Roy, S., Edmonds, D.A., 2017. Land loss by pond expansion on the Mississippi River Delta Plain. Geophys. Res. Lett. 44 (8), 3635–3642.
- Ou, Y., Xue, Z.G., Li, C., Xu, K., White, J.R., Bentley, S.J., Zang, Z., 2020. A numerical investigation of salinity variations in the Barataria estuary, Louisiana in connection with the Mississippi River and restoration activities. Estuar. Coast. Shelf Sci. 245 (107), 021.
- Palaseanu-Lovejoy, M., Kranenburg, C., Barras, J.A., Brock, J.C., 2013. Land loss due to recent Hurricanes in coastal Louisiana, USA. J. Coast. Res. (63 (10063)), 97–109.
- Paola, C., Twilley, R., Edmonds, D., Kim, W., Mohrig, D., Parker, G., Viparelli, E., Voller, V., 2011. Natural processes in delta restoration: Application to the Mississippi Delta. Annu. Rev. Mar. Sci. 3, 67–91.
- Papin, P., Berg, R., 2022. National Hurricane Center Tropical Cyclone Report: Tropical Storm Claudette. Al032021, National Oceanic and Atmospheric Administration, National Weather Service, Washington, DC.
- Paron, P., 2014. Hydro-Meteorological Hazards, Risks and Disasters. Academic Press.

- Pasch, R., Berg, R., Roberts, D., Papin, P., 2021. National Hurricane Center Tropical Cyclone Report: Hurricane Laura. Al132020, National Oceanic and Atmospheric Administration.
- Payandeh, A., Justic, D., Mariotti, G., Huang, H., Sorourian, S., 2019. Subtidal water level and current variability in a bar-built estuary during cold front season: Barataria Bay, Gulf of Mexico. J. Geophys. Res.: Oceans 124 (10), 7226–7246.
- Ren, L., Nash, S., Hartnett, M., 2015. Observation and modeling of tide-and wind-induced surface currents in Galway Bay. Water Sci. Eng. 8 (4), 345–352.
- Shashank, V., Mandal, S., Sil, S., 2021. Impact of varying landfall time and cyclone intensity on storm surges in the Bay of Bengal using ADCIRC model. J. Earth Syst. Sci. 130 (4), 1–16.
- Sheremet, A., Mehta, A., Liu, B., Stone, G., 2005. Wave–sediment interaction on a muddy inner shelf during Hurricane Claudette. Estuar. Coast. Shelf Sci. 63 (1–2), 225–233
- Siverd, C.G., Hagen, S.C., Bilskie, M.V., Braud, D.H., Peele, R.H., Foster-Martinez, M.R., Twilley, R.R., 2019. Coastal Louisiana landscape and storm surge evolution: 1850–2110. Clim. Change 157 (3), 445–468.
- Sorourian, S., Huang, H., Li, C., Justic, D., Payandeh, A.R., 2020. Wave dynamics near Barataria Bay tidal inlets during spring-summer time. Ocean Model. 147 (101), 553.
- Swarzenski, C.M., et al., 2003. Surface-Water Hydrology of the Gulf Intracoastal Waterway in South-Central Louisiana, 1996-99. US Department of the Interior, US Geological Survey.
- Turner, R.E., Layne, M., Mo, Y., Swenson, E.M., 2019. Net land gain or loss for two Mississippi River diversions: Caernarvon and Davis Pond. Restoration Ecol. 27 (6), 1231–1240.
- Valentine, K., Mariotti, G., 2019. Wind-driven water level fluctuations drive marsh edge erosion variability in microtidal coastal bays. Cont. Shelf Res. 176, 76–89.
- Vijayan, L., Huang, W., Yin, K., Ozguven, E., Burns, S., Ghorbanzadeh, M., 2021.
  Evaluation of parametric wind models for more accurate modeling of storm surge:
  A case study of Hurricane Michael. Nat. Hazards 106 (3), 2003–2024.
- Webster, P.J., Holland, G.J., Curry, J.A., Chang, H.-R., 2005. Changes in tropical cyclone number, duration and intensity in a warming environment. Science 309 (5742), 1844–1846.
- Wilson, M., Meyers, S., Luther, M.E., 2006. Changes in the circulation of tampa bay due to Hurricane Frances as recorded by ADCP measurements and reproduced with a numerical ocean model. Estuar. Coasts 29 (6), 914–918.
- Xu, K., Bentley, S.J., Day, J.W., Freeman, A.M., 2019. A review of sediment diversion in the Mississippi River deltaic plain. Estuar. Coast. Shelf Sci. 225 (106), 241.
- Young, I.R., Verhagen, L., 1996. The growth of fetch limited waves in water of finite depth. Part 1. Total energy and peak frequency. Coast. Eng. 29 (1-2), 47-78.
- Yuill, B., Lavoie, D., Reed, D.J., 2009. Understanding subsidence processes in coastal Louisiana. J. Coast. Res. (10054), 23–36.
- Zhao, H., Chen, Q., 2008. Characteristics of extreme meteorological forcing and water levels in Mobile Bay, Alabama. Estuar. Coasts 31 (4), 704–718.